Development of a modular mooring system with clump weights

Giovanni Rinaldi [1]*, Tessa Gordelier [1], Mark Sansom [2] and Lars Johanning [1, 3]

[1] Renewable Energy group at the University of Exeter, Penryn Campus, Treliever Road, TR109FE, Penryn, Cornwall, UK; g.rinaldi@exeter.ac.uk, t.j.gordelier@exeter.ac.uk, l.johanning@exeter.ac.uk
[2] Falmouth Harbour Commissioners, 44 Arwenack Street, TR11 3JQ, Falmouth, Cornwall, UK; hm@falmouthharbour.co.uk
[3] College of Shipbuilding Engineering, Harbin Engineering University, Harbin, 150001, China

*** Correspondence:**
Giovanni Rinaldi
g.rinaldi@exeter.ac.uk

Keywords: Mooring system, hybrid anchors, clump weights, Falmouth Harbour, Orcaflex

Abstract

Mooring systems constitute a fundamental component of all floating systems. For port authorities and device developers, improvements in moorings and foundations allow for savings in capital costs and increased revenues. In this work, a cost effective and secure mooring system for the station keeping of commercial vessels is presented and developed. A modular arrangement constituted by a series of connecting lines and clump weights is proposed, in order to allow for its deployment by small or craft vessels, and reduce the capital, installation and maintenance costs with respect to those of traditional mooring systems. The mooring system is calibrated according to the environmental conditions of Falmouth Harbour, UK. A numerical model of the mooring system is implemented using the offshore dynamics analysis software OrcaFlex. Experimental demonstration is provided through testing of a scaled prototype. Both numerical and experimental investigations aim at a preliminary evaluation of the design proposed. The outcomes indicate the feasibility of the arrangement as a suitable alternative to conventional and more expensive mooring systems. Further areas of improvement are identified and outlined.

1 Introduction

Most watercrafts require the use of a mooring system in order to securely hold position for extended periods of time. The primary role of moorings is to keep a structure in place and allow it to withstand the loads generated by environmental factors (e.g. wind, waves and currents) as well as potential impact with external bodies (e.g. ice blocks). As such, among their shipping related services, many commercial harbours provide mooring infrastructure such as swinging moorings. However, the installation and maintenance of these systems has a significant cost, and poses a number of technical challenges especially in relation to the durability and reliability of the station-keeping under harsh weather conditions. Besides, due to the increasing penetration of offshore renewable energy (ORE) devices in the energy production industry, innovative and specific mooring systems [1,2] developed using suitable software packages and design tools [3] are needed.

In the instance of wave energy converters (WECs), the mooring systems can be an integral part of the power conversion mechanism with very specific requirements. Additionally, to realise the full potential of floating offshore wind, reductions in capital cost of infrastructure will be required through mooring system innovations [4]. Therefore, despite the existence of a number of conventional approaches and standard configurations [5,6], novel moorings and foundations arrangements are frequently developed, either for a generic floating body and site, or for a specific class of floating structures and environmental conditions.

Generally, when a mooring system is conceived, three main aspects are considered [7]: the motions of the watercraft, the resulting tension on the mooring lines and the anchors' holding capacity. A dedicated work of balance and calibration among these three aspects is required in order to produce a safe design while ensuring economic feasibility.

In this work, a novel solution for a cost effective and modular mooring system, which can be used for secure mooring of ORE devices as well as large floating bodies (e.g. commercial vessels and cruise liners), is developed. The main innovation of the proposed arrangement consists in the efficacy, modularity and cost-effectiveness of the mooring concept with respect to traditional configurations exploiting heavy and bulky components. This is specifically designed for Falmouth Harbour, located in the south west of the United Kingdom, where, the limited water depths prevent the berthing alongside the quayside. The novel mooring system could be used to increase the current mooring infrastructure capabilities of the harbour, consisting of an admiralty swinging mooring suitable for vessels up to 180m long and up to 10.5m draught. A mooring system of this kind costs in the order of £350,000 for capital expenditures alone, to which installation and maintenance costs have to be added. The first can be estimated at around £200,000, due to the 4-days charter of an appropriate anchor handling vessel at approximately £50,000/day. The second can be estimated at around £20,000 every 3 to 5 years, due to the contracting of divers and related support vessel to maintain the mooring system components.

Under these premises, the desired requirements of the mooring system and foundations were established in agreement with the indications of Falmouth Harbour Commissioners (FHC), the local port authority [8], as follows:

- Capable of holding vessels on station across the range of environmental conditions that a ship can experience at Falmouth Harbour. The environmental characteristics of the site (shown in Table 1) were provided by FHC;
- Achieve a maximum effective tension of the mooring lines of 150 tons (~1500kN). This limit was established in accordance with the values registered with the existing mooring system already installed in Falmouth Harbour;
- Where possible, use cost-effective components and materials, such as synthetic ropes as a cheaper alternative to more expensive steel chains. In this regard, the use of synthetic ropes for permanent mooring systems is well reviewed and documented in [9,10]. Synthetic or polymeric ropes are light, flexible, and can provide large restoring forces [11,12]. However these are traditionally less employed than ropes or chains;
- Adopt a modular design, including redundancy in case of line failures;
- Able to be connected to a standard surface mooring buoy, identical to the one in the existing mooring configuration. The moored vessel is able to connect to the large ring on top of the buoy using ropes or chain;

- Utilise clump weights having a maximum weight of 4 tons and a maximum volume of $2m^3$. The use of clump weights in mooring systems has been already investigated in literature [7,11,13]. The main rationale for their utilization is the minimization of the vertical loads at the end of the mooring lines, which in turn reduce the uplifting forces (and therefore holding requirements) on the anchors. In this way, a cheaper alternative to the bulky embedment anchor used in the existing mooring system can be proposed. The same strategy is also used for guyed towers, offshore structures held in place by a symmetric array of catenary guylines whose lower parts possesses clump weights which are lifted off the bottom during heavy seas [14];
- Allow for the utilization of the small craft vessels and workforce already available at Falmouth Harbour for all installation, maintenance and decommissioning activities. In this way charter and subcontracting costs are reduced and the safety of the operations increased; and
- Minimize environmental impacts, by using non-invasive installation techniques, smaller components and local materials.

Table 1. Environmental and site constraints used for the mooring system design.

Parameter	Value
Water depth	25 m
Significant wave height	2 m
Wave mean period	6 s
Current speed	0.45 m/s
Wind speed	45 m/s
Seabed type	Sand

Thus, according to the desired requirements described above and the values shown in Table 1, a novel mooring system is firstly developed numerically in Orcaflex and then tested (at reduced scale) for experimental demonstration. In this regard, it must be noticed that both the numerical and experimental modelling works are a preliminary investigation aiming at receiving useful feedback on the feasibility and future improvement of the system. Although, for practical reasons and demonstration purposes, a model ship is used as the moored watercraft in both the numerical and experimental modelling shown in this work, an offshore renewable device (e.g. a wave energy converter or a floating offshore wind turbine) could be used instead. The rest of this paper is organized as follows. In section 2, the methodology followed to achieve the final design of the mooring system is provided. In section 3, the relevant results obtained for both the numerical and experimental phases are provided. These outcomes are discussed in view of the proposed application,

together with possible weaknesses and areas of improvement, in section 4. Finally, conclusions are drawn and proposal for future work outlined in section 5.

2 Methodology

2.1 Phase 1 - Numerical modelling

After a background research to identify existing solutions, the first step of the mooring system development consisted in a preliminary feasibility assessment, based on the station keeping simulation performed in specific computational software. OrcaFlex [15], a robust and validated software package for the dynamic analysis of offshore marine systems (including mooring systems and ships dynamics) was selected for this purpose. This was also identified as a relevant tool for such investigations in previous literature conducting a screening of available tools for dynamic mooring analysis [16]. A set of sea states reproducing the harshest environmental conditions available at Falmouth Harbour, as indicated in Table 1, were recreated in the simulation. To maximize the environmental loading, the wind, wave and current loads were aligned in the same direction, with the vessel able to weathervane. The environmental loads direction, as well as wind and current profile in height and depth, were kept constant during the simulations. An iterative process, evaluating motions of the vessel and of the clump weights, as well as tensions on the mooring lines, was used in order to establish the appropriate number and characteristics of the mooring lines. Materials and properties of the mooring lines were defined according to the specifications provided by FHC for the existing mooring system components, or retrieved by online catalogues provided by components manufacturers [17,18] for any additional components selected for the novel mooring system. For the sake of the simulation, hypothetical heavy masses were used instead of anchors at the end of each mooring line. This allowed for the estimation of the holding requirements of the anchors. Both static and dynamic simulations were run until convergence in the design was reached. A total time of 3600s (1 hour) is shown in the dynamic simulation outputs in the next sections. After checking with longer simulation times (up to 3 hours), this is chosen as a satisfactory period to make sure that the build-up stage (environmental loads steadily increasing to their final size) is concluded, and all relevant phenomena have been captured. This means that, also due to the moderate environmental conditions simulated, the second and higher order responses are fully developed, eventual extreme events are detected, and the trends of monitored results have not changed significantly over the last third of the simulation. The simulation parameters are provided in Table 2, and spectra of the environmental loads shown in Figure 1.

Table 2. Setup parameters used for the simulation in OrcaFlex.

Parameter	Value
Wave spectrum	Jonswap
Environmental conditions	As indicated in Table 1
Ship length (waterline)	150 m

Ship mass	13133 tons
Ship height	19 m
Ship draught	9.7 m
Simulation time	3600 s

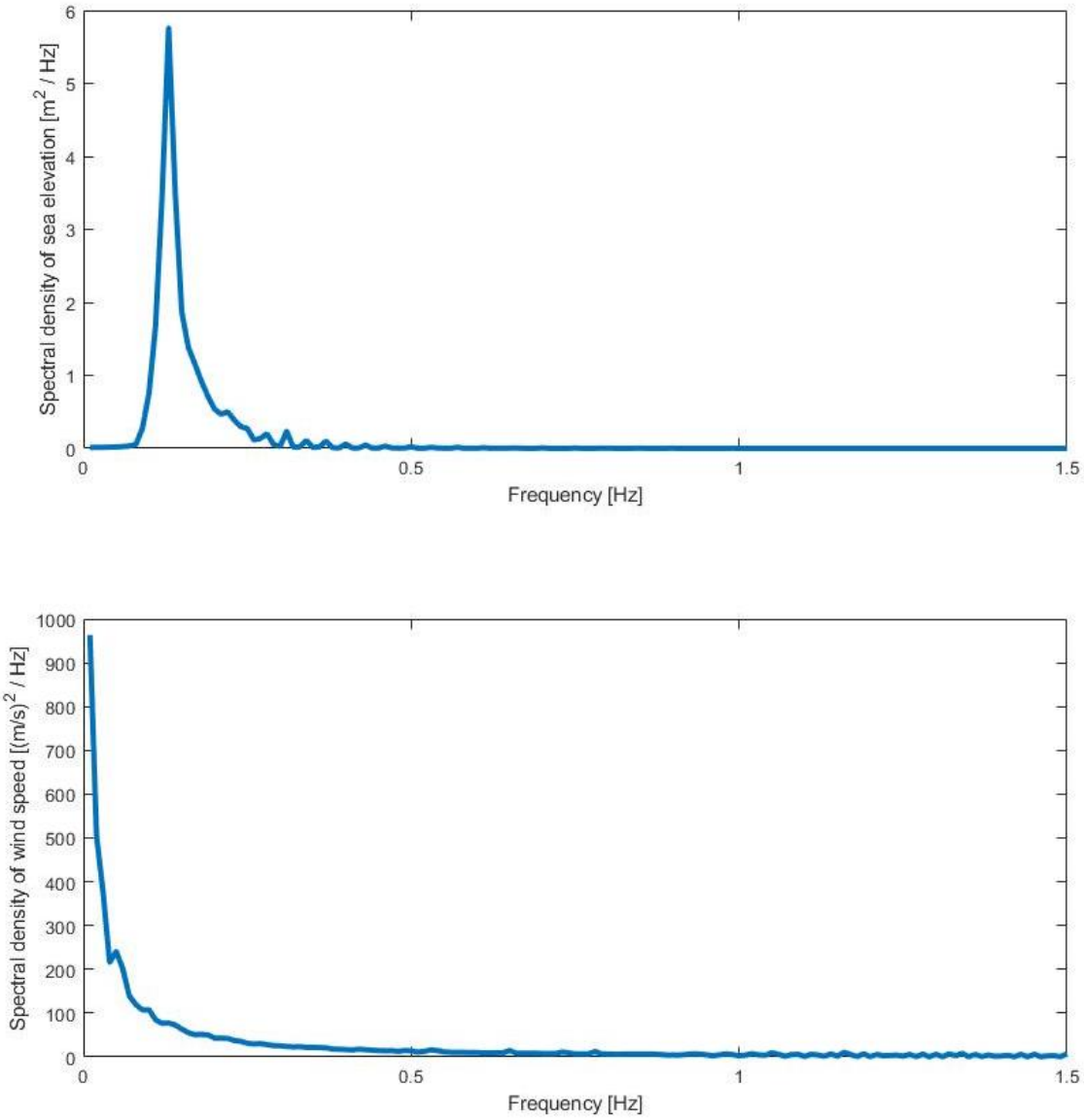

Figure 1. Spectra of the environmental loads generated in the Orcaflex model. Wave spectrum (top), Wind spectrum (bottom). Current is constant.

Mooring systems should be designed to withstand first (linear), second and higher (non-linear) order loads. Since the motion characters will influence the dynamic responses of the mooring system, as well as to facilitate the reproducibility of this work, the hydrodynamic response characteristic of the vessel used in the analyses is shown through the response amplitude operators (RAOs) curves in Figure 2 and the spectral response in Table 3, both calculated using Orcaflex. The vessel has been defined by selecting one of the vessel types already available in the Orcaflex library, and its size adjusted to represent a large ship anchored at Falmouth harbour. The dynamic response of the ship is calculated based on dynamic motion equation considering the hydrodynamic loads acting on structure, including the first order wave force, second order drift force, wind force and current load. It should be noted that the hydrodynamic parameters in the dynamic motion equation are usually imported from external sources. As explained in the Orcaflex documentation, "if the vessel length

differs from the vessel type length then the RAO periods given on the vessel type form are Froude scaled".

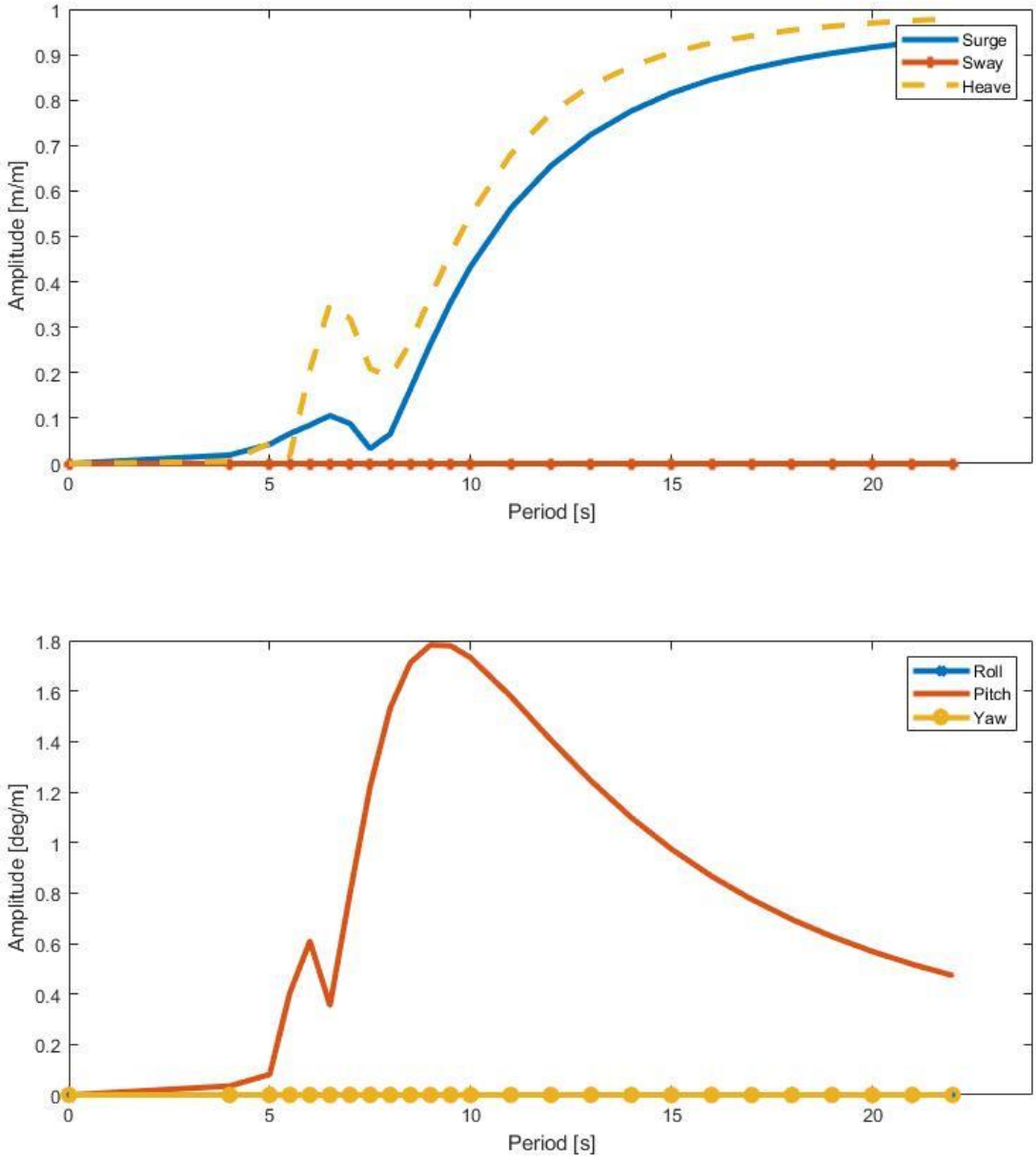

Figure 2. Response amplitude operators (RAOs) of the vessel modelled in Orcaflex.

Table 3. Spectral response of the moored vessel modelled in Orcaflex.

	Surge (m)	**Sway** (m)	**Heave** (m)	**Roll** (deg)	**Pitch** (deg)	**Yaw** (deg)	**Z above wave** (m)
Significant amplitude	0.13131	0	0.252464	0	1.126677	0	0.967126
3 hour max amplitude	0.247706	0	0.480399	0	2.138531	0	1.875248

Average period (s)	8.759702	N/A	7.734448	N/A	8.019111	N/A	5.858739

2.2 Phase 2 – Experimental investigation

Following the preliminary feasibility study, an experimental demonstration of a scaled prototype of the mooring system was conducted. This was not intended as a validation of the numerical model in its classical meaning, as described in [19,20]. A series of tests were conducted in the wave tank available at Plymouth COAST laboratory [21], in order to extend the results obtained with the numerical model as well as to gain further insights on the effectiveness of the overall design. The experimental tests consisted in evaluating the performance of the scaled mooring system under a range of waves and current conditions.

The setup and outcomes of both the numerical and experimental phases are individually described in the next section.

3 Results

3.1 Phase 1 - Numerical modelling

The mooring design proposed according to the considerations explained in the above sections is shown in Figure 3. This is obtained at the end of an iterative procedure, which consisted in adding, removing or modifying the different constituents of the mooring systems according to the outcomes of each simulation, monitoring especially the tension acting on the various mooring lines. As such, the objective of the iterative procedure was to reach a stable and effective configuration according to the requirements initially listed in the introduction. This could be also interpreted as a multi-objective optimization problem under a series of constraints, such as the minimization of parts/materials (hence costs) while also the tension measured on the mooring lines is minimized. The final arrangement includes a series of eight mooring lines. All mooring lines converge towards a central steel ring, already used in the existing mooring configuration, laying on the seabed (in absence of external loads). In this way, the tension is effectively spread among all mooring lines under the action of environmental loads. The steel ring is then connected to a mooring buoy, modelled on the basis of the existing configuration, by means of a 4″ studless chain. The mooring lines are symmetrically distributed with respect to one central line, which lies on the same direction of the environmental loads (waves, wind and current). It is thus assumed that, in case of deployment, an orientation of the mooring system will have to be chosen according to the prevalent direction of loads in Falmouth Harbour area. Accordingly, the mooring lines are more concentrated (minor angle between two consecutive lines) on the side of the predominant loading, with mutual angles of 20°, 40° and 60° respectively. Similarly, the number of clump weights (indicated by the blue dots in Figure 1) varies according to the same criterion: 6 weights on the side of predominant loading, then 5 in all the other lines except the mooring line opposite the prevalent loading direction, which has 4 weights. The clump weights vary in weight according to their distance from the central ring: 2 tons for the first one (the closest one to the central point), 3 tons for the second, and 4 tons for all the other ones. This variation in weights favours the obtainment of a catenary behaviour of the mooring lines when these are pulled because of the vessel's motions. The clump weights are modelled as cubes of different sizes according to the properties of granite, a material chosen due to its limited cost, its high density (~2750 kg/m3) and its wide availability in Falmouth area. All clump weights are attached to the

mooring lines at uniform intervals of 30m. Each of the mooring line sections is a synthetic rope based on the Dyneema SK78 properties [17], and is connected to the clump weights at least 1m above the seabed, in order to reduce friction and subsequent deterioration. Even if more sensitive to degradation, synthetic ropes are generally cheaper to buy, install and especially to maintain. This means that even if they would need replacement more often than other materials (e.g. steel chains), this higher frequency would be mitigated by the lower capital cost of the material and especially by the lower requirements for vessels, tools (e.g. cranes) and work force. The complete specifics of the mooring design proposed are detailed in Table 4.

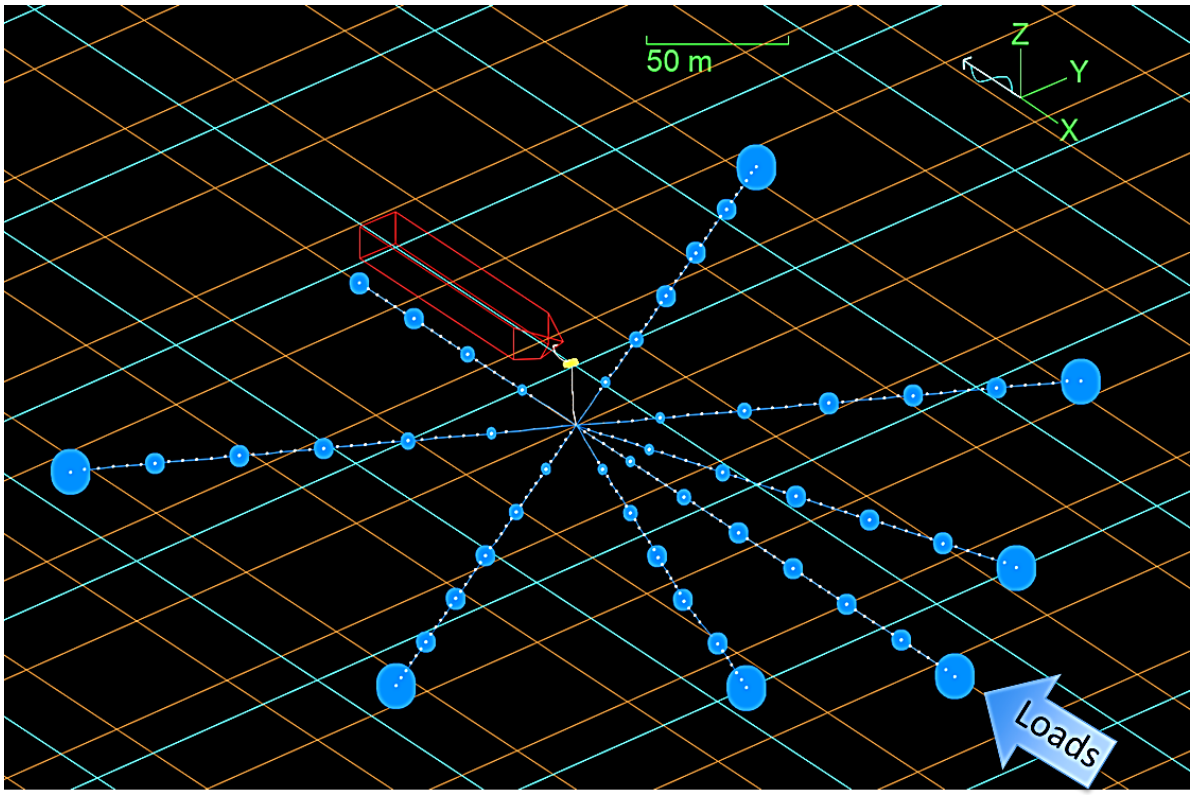

Figure 3. OrcaFlex representation of the implemented mooring system. Lateral view.

As mentioned in the previous section, the outermost blue dots at the end of the mooring lines in Figure 3 represent fictitious clump weights used to calculate the required holding power of the anchors. The mass of these weights was gradually increased until a stable configuration is reached (i.e. the ends of the mooring lines are not dragged away as a consequence of the incoming loads). Thus, a final mass of around 70 tons per fictitious clump weight is needed in order to satisfy this requirement.

Table 4. Specifics of the mooring design proposed.

Parameter	Value
Chain connecting mooring buoy to central ring	24 m long, 0.1m ø studless chain, 0.198 t/m

Hawser connecting ship to mooring buoy	15m long, 0.1m ø rope, 0.0052 t/m
Mooring buoy	4.8m long, 2.4m ø, 5.25 tons
Synthetic mooring line sections	30 m, 0.1m ø Dyneema SK78 rope, 0.0042 t/m, 9769 kN axial stiffness, 0.008 axial drag coefficient, no damping, 0.78 seabed friction coefficient
Clump weights mass	2 / 3 / 4 tons
Clump weights volume	0.73 / 1.09 / 1.45 m^3
Clump weights density	2750 kg/m^3
Clump weights-seabed friction coefficient	0.55

Note: values for the clump weights refer to the 1st (2 tons), 2nd (3 tons) and 3rd to last weight (4 tons) respectively (starting from the central ring and moving towards the anchor end of the mooring line).

Once the simulations are run, a series of results can be analysed to verify that the conditions initially proposed are respected. For example, when the tension of the mooring line positioned opposite to the vessel (because this is the one experiencing the highest loads) is measured, the results shown in Figure 4 are obtained. Here, it can be seen that the maximum tension allowed as an initial design requirement (150tons, 1500kN) is respected, with maximum values of around 400kN.

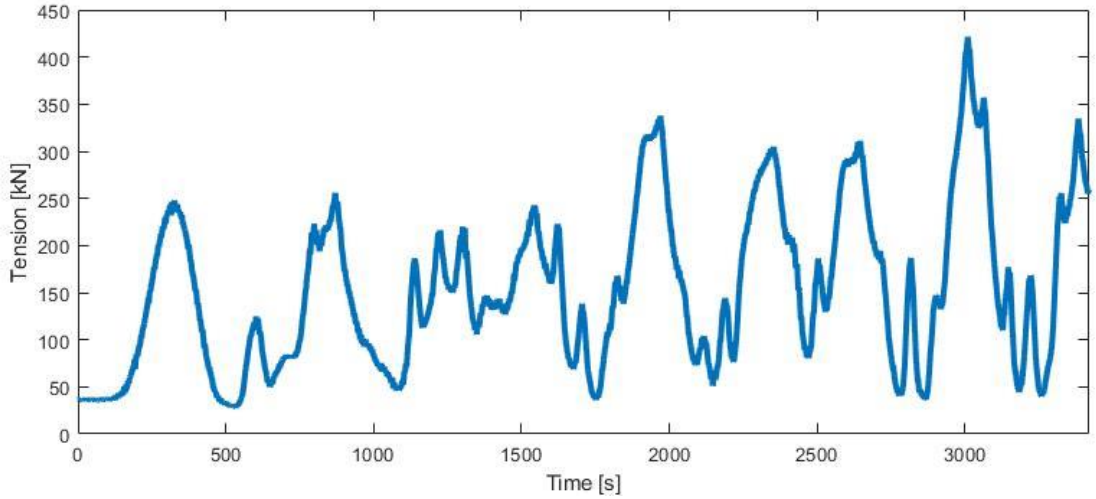

Figure 4. Tension on the mooring line facing the vessel during the dynamic simulation.

However, the moderate tension comes at a price. In fact, when the motions of the moored vessel are analysed (Figure 5), a significant excursion of up to 45m in surge can be noticed. This can be somehow expected as a consequence of the synthetic material chosen for the mooring lines, which

provides lower restoring force when compared against other materials (e.g. steel chains). Nonetheless, no limiting criteria for acceptable displacements are considered at this stage.

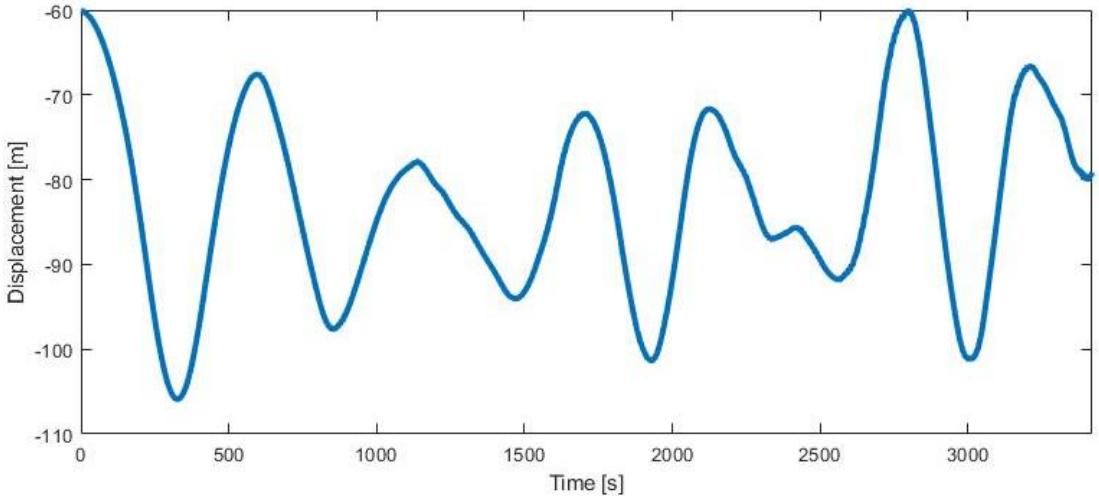

Figure 5. Motion response of the vessel in surge during the dynamic simulation.

3.2 Phase 2 – Experimental demonstration

Following the concept design, a prototype of the mooring system in scale 1:30 was built in order to verify the results of the numerical modelling and obtain further indications for its development. This scaling was chosen according to the dimensions of the wave tank used for the experiment and practical aspects related to the downscaling of all the mooring system components. The components of the mooring system, as well as the vessel and the testing environment (including simulation time), were scaled using Froude scaling. Due to practical reasons, an accurate downscaled version of the synthetic rope could not be found. Therefore, a commercial solution matching as much as possible the description of the Dyneema material chosen for the mooring lines, was selected for the experimental set-up. Similarly, due to budget and time constraints, an accurate downscaled version of the vessel was not manufactured. A pre-existing model vessel was used instead, considering that it had very close mass and dimension values to that of the numerically modelled vessel, and that if needed it would have been quicker/cheaper to change the vessel in the numerical model. This is also one of the reasons why validation between numerical and experimental models in its strict sense was not sought. Besides, since firm requirements on the vessel to be moored were not defined (because the mooring system principle is proposed for a generic range of ships and/or ORE devices), major focus was put in obtaining a reliable downscaling of the mooring system, which is the main object of this investigation.

The arrangement for the experimental test is schematized in Figure 6. Here, lead weights (in grey) are used to resemble the massive clumps at the end of the mooring lines (representing the anchors) and to fix the mooring lines to the floor. The granite clump weights of different mass are shown in blue, and the load cells used to measure the loads on different sections of the mooring lines (numbered from 0 to 5 depending on their position) in red. Given that the model and full scale granite clump weights have the same density, Froude scaling of volume was carried out to make sure that model scale and full scale weights are comparable. The floater to which the model ship was connected, representing the mooring buoy on the water surface, is represented in yellow. A series of five wave gauges, positioned at different distances from the wave-makers and parallel to the wave tank sidewalls, is used to measure the waves' properties, a flow meter to measure the water current properties and a

motion detection system to measure the movements of the model ship. An overview of the experimental setup as seen from the cameras installed to monitor the system (but not to measure underwater motions) is provided in Figure 7.

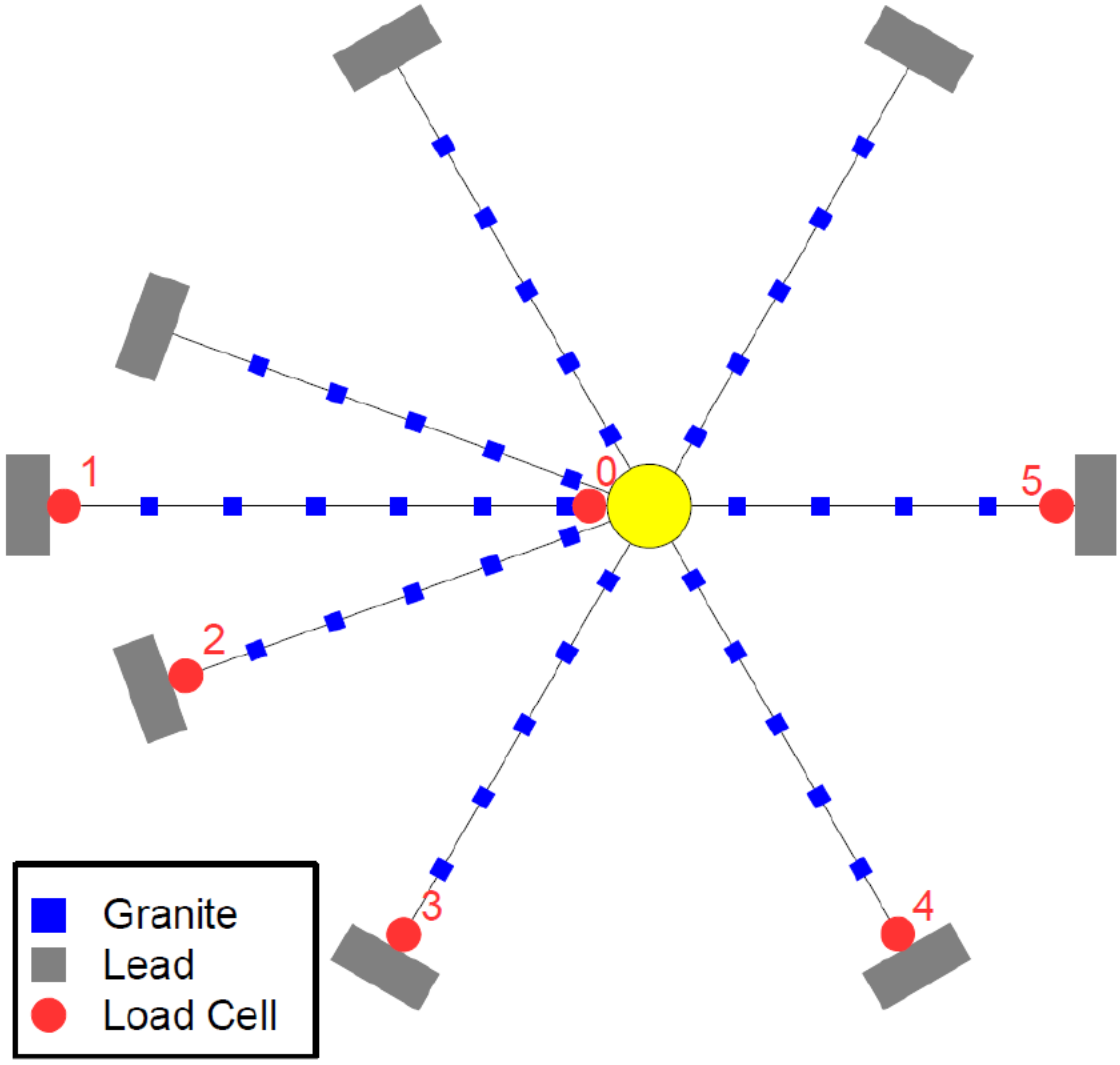

Figure 6. Mooring system arrangement for experimental tests. In this scheme, waves and/or currents come from the left hand side.

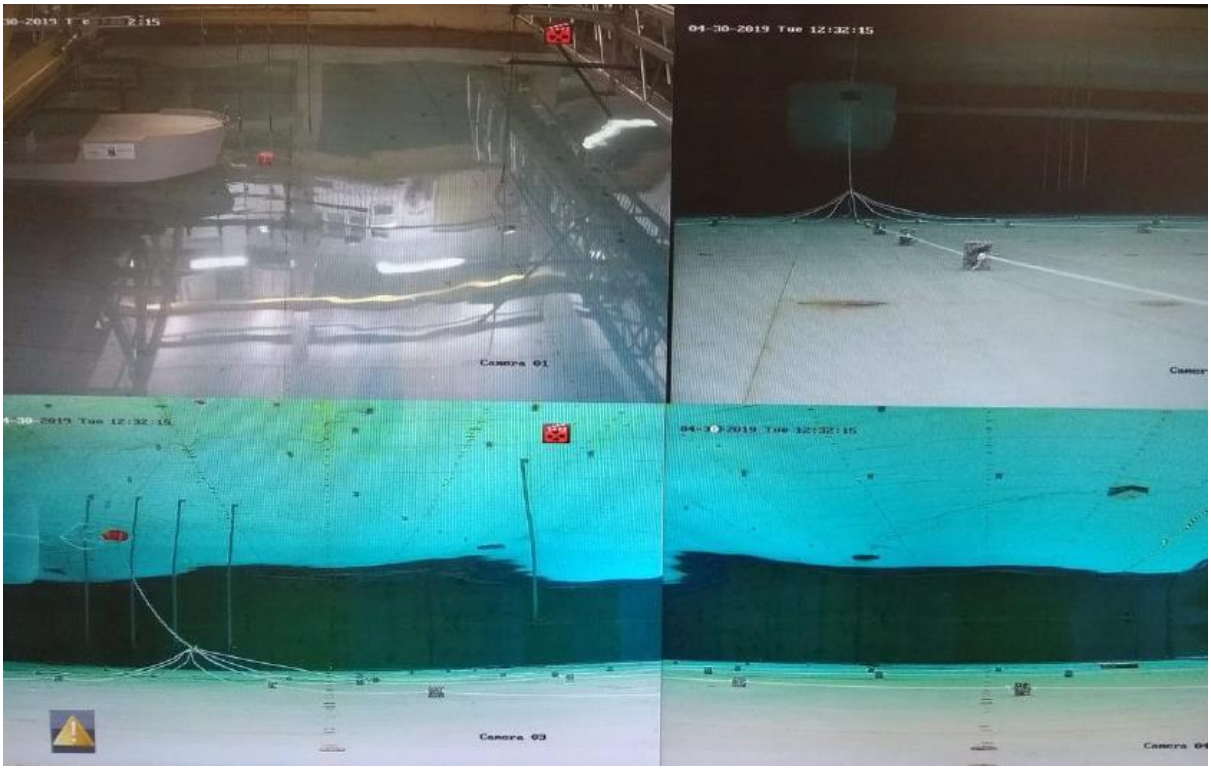

Figure 7. Overview of the experimental setup from cameras (one above and three under water). Model ship attached to the mooring buoy (top left), centre of the mooring system and granite clumps interconnected by synthetic strings (top right and bottom left), and end of one of the mooring lines (bottom right).

The objective for this second phase was the evaluation of loads generated on the mooring lines. Also the motions of the mooring legs were examined qualitatively by using underwater cameras. Due to the impossibility of generating wind in the wave tank available, only the effect of waves and current were verified.

Thus, a total of 60 test cases with both regular and irregular waves alone, currents, and waves and currents combined, was considered. Specifically:

- Runs 1-31 involved the use of *regular waves only*. The wave height (at full scale) was kept at 1.2m, while the period ranged from 4s to 10s with an increment of 0.2s;
- Runs 32-37 involved the use of *irregular waves only*. The significant wave height H_S (at full scale) ranged from 1.2m to 2.6m (0.4m increment) and the mean zero up-crossing period T_Z from 4s to 9s (1s increment);
- Runs 38-51 and Run 60 involved the use of *irregular waves with currents*. The same conditions of Runs 32-37 were tested, with the addition of 0.3m/s and 0.45 m/s (at full scale) currents. For Run 60 the current was set at 1.3m/s; and
- Runs 52-59 involved the use of *currents only* ranging from 0.54m/s to 2.47m/s (at full scale).

All the characteristic values for each run of these tests, both at model and full scale (using Froude scaling), are shown in Tables A1 – A4 in Appendix.

The data collected during the tests included feedback measurement on waves and currents generated. However, the source of information of major interest for the investigation of the mooring system were provided by:

- the loads recorded by the load cells positioned in different points of the mooring lines;
- the motions of the model ship in terms of its six degrees of freedom (DOFs), measured through a rigid body calculation based on multiple markers.

Therefore, due to the higher number of cases tested in this phase, the overall results were initially analysed in comparison to each other for both these two sets of parameters. The results of this comparison are shown in the boxplot and bar graphs in Figure 8 Figure 11.

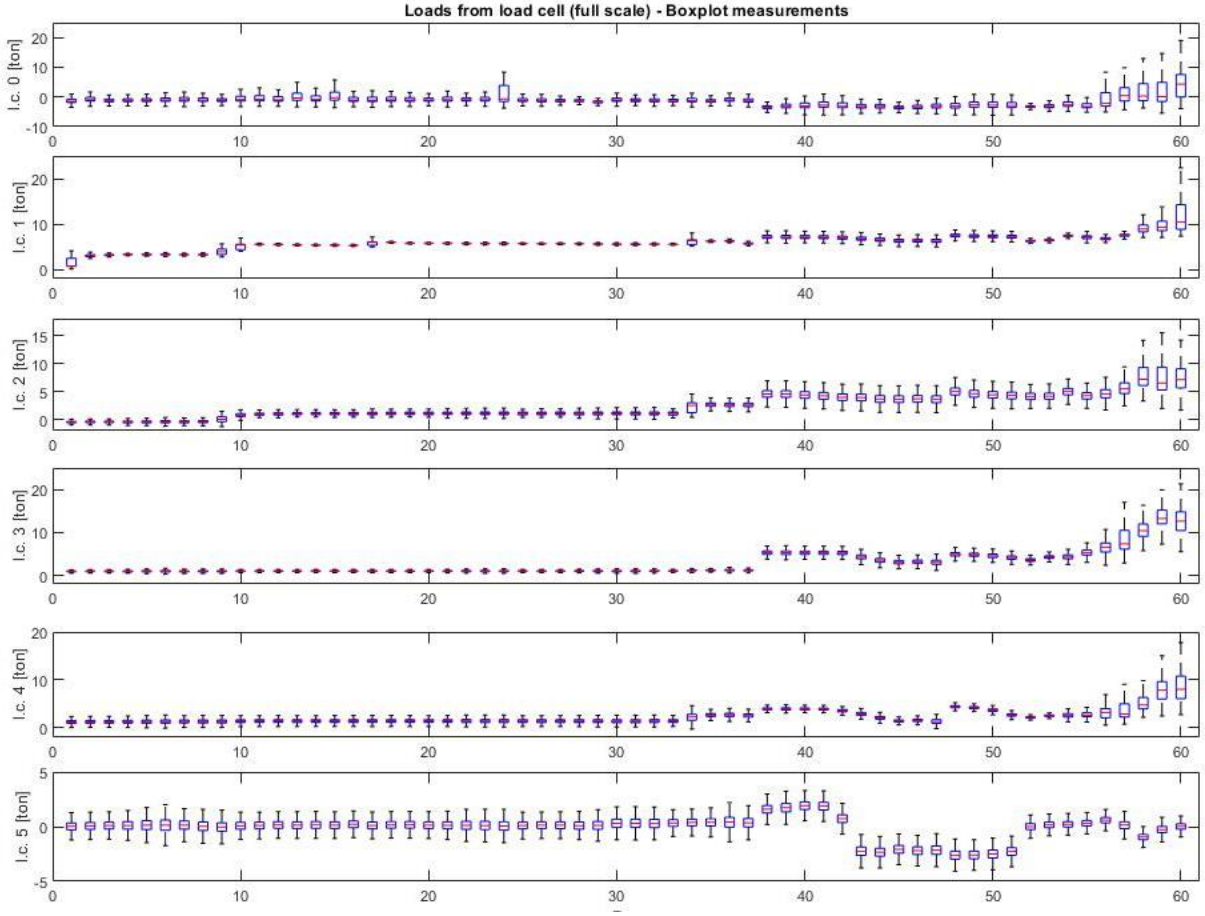

Figure 8. Boxplot of the loads recorded for each run by each load cell (noted as l.c. in the y-axis) during the experimental tests.

Figure 8 shows the boxplot of each series of measurements during the tests. On each box, the central mark indicates the median, and the bottom and top edges of the box indicate the 25th and 75th percentiles respectively. The whiskers indicate the most extreme data points not considered outliers.

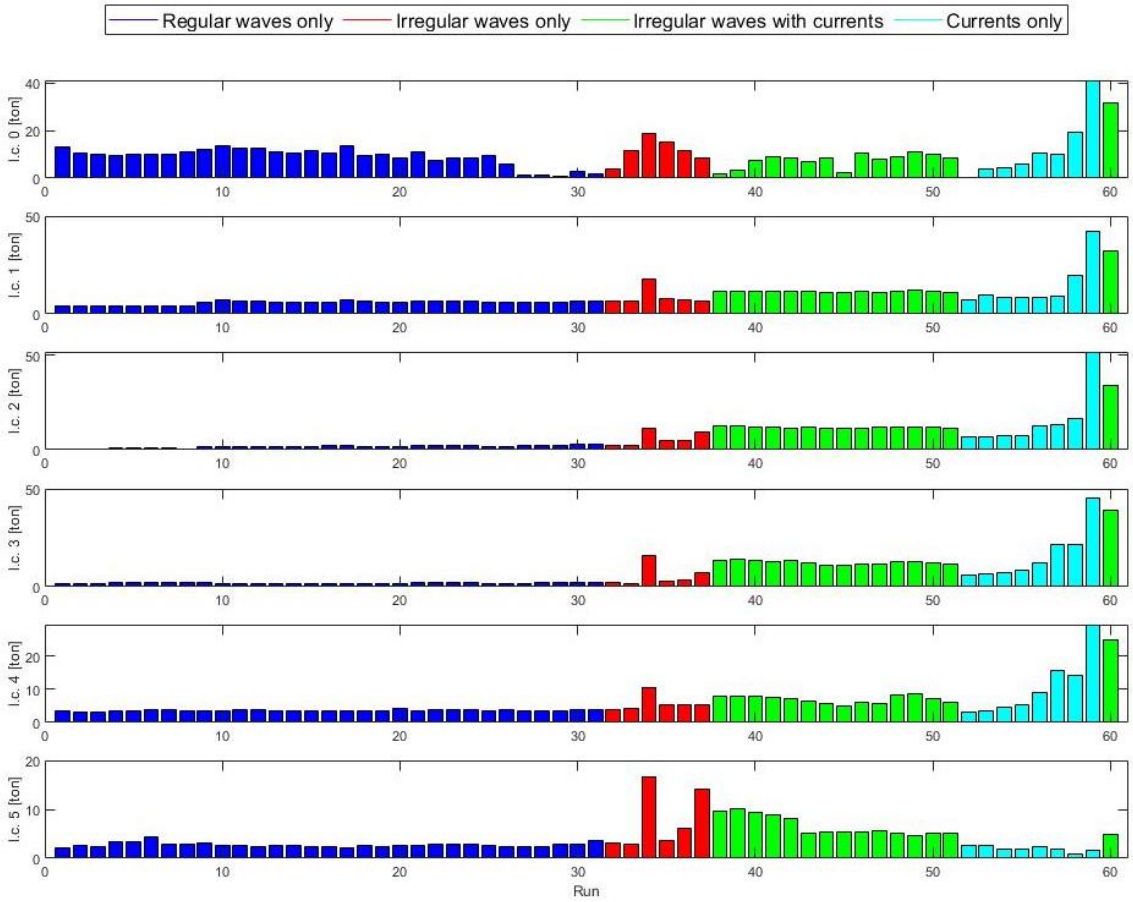

Figure 9. Maximum load recorded for each run by each load cell (noted as l.c. in the y-axis) during the experimental tests.

Figure 9 shows the maximum load, scaled up to full scale values, measured by each one of the six load cells during the tests. Here it can be seen how the loads generally tend to decrease from the load cell 0 (the closest to the central ring and floater) to load cell 5 (the one positioned on the opposite direction with respect to the coming waves and currents). Besides, the loads tend to be higher for those cases in which current is applied. In this regards, it must be taken into account that in the last cases with current only (Run 60) the intensity was increased on purpose, beyond realistic values previously modelled numerically, in order to compensate for the lack of wind during the tests. However, this result confirmed that the highest loads are generated by the action of current rather than by that of waves. In addition, all the measured loads (at full scale) were below 60 tons, meaning that the mooring system is working effectively in holding the model ship in position without generating excessive loads on the end of the mooring lines where the anchors will be placed. Finally, from this graph it can be seen that the most critical cases in terms of loads are the runs number 34, for the situation with irregular waves only, and number 59, for the case with currents only. These values and load distribution among the mooring lines are consistent with the expectations from the numerical model.

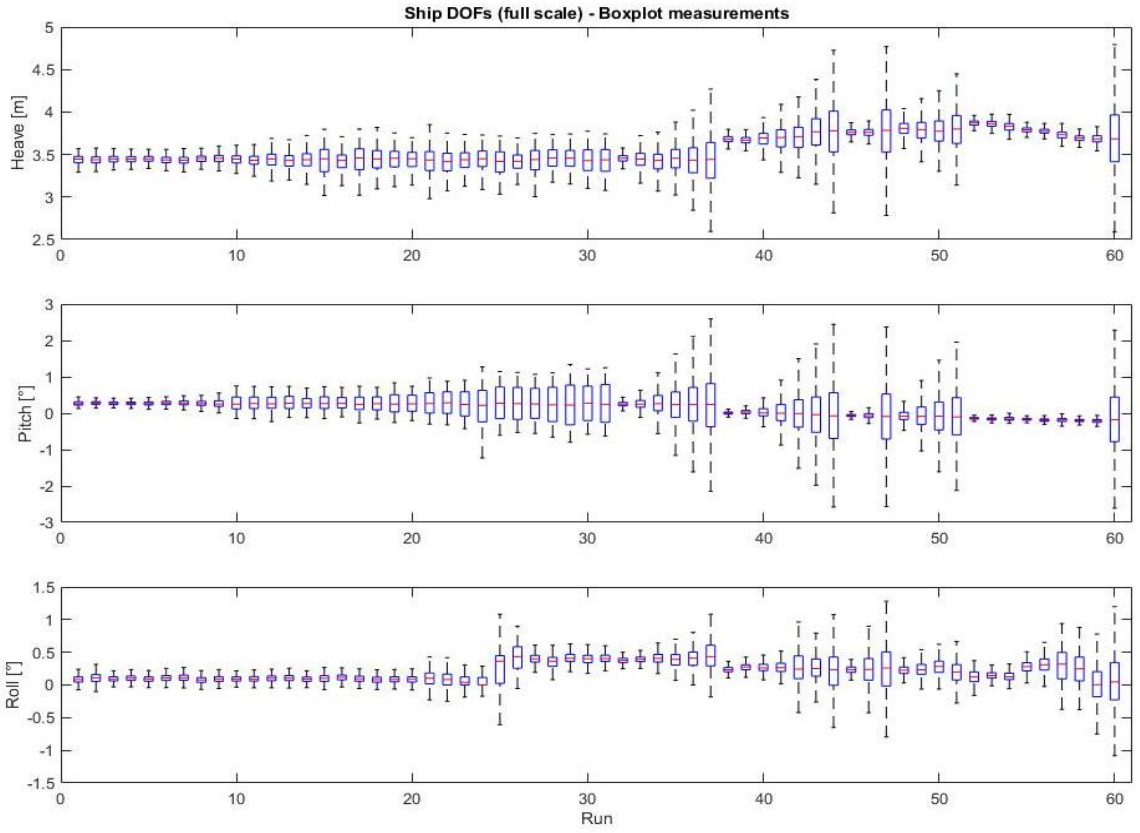

Figure 10. Boxplot of the motions of the model ship for heave, pitch and roll during experimental tests.

In Figure 10, the boxplots of the motions of the model ship measured during the experimental tests for heave, pitch and roll, are shown. Also in this case, the red mark at the centre of each box indicates the median, while the bottom and top edges indicate the 25th and 75th percentiles respectively and the whiskers indicate the most extreme data points not considered outliers. This allows to show more of the dynamic information of the measurements.

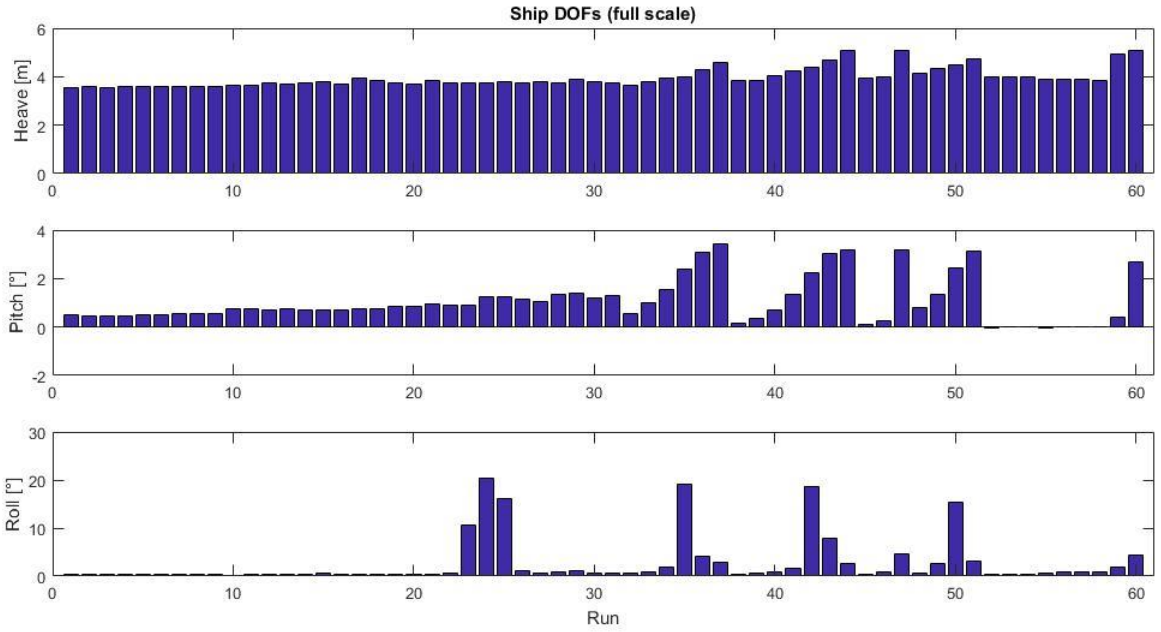

Figure 11. Maximum motions of the model ship for heave, pitch and roll during experimental tests.

Figure 11 shows the data related to three of the six registered DOFs for the model ship (heave, pitch and roll). The maximum variation for each of these three DOFs is reported for each test case. The motions for these specific DOFs were chosen for further analysis because their variations follow a symmetric oscillatory trend (this is better displayed in Figure 12 Figure 15), therefore it is easier to extrapolate a maximum variation. From Figure 11 it appears that the run cases producing the greatest motions are not the same as the cases that generated the highest mooring line loads, previously identified when the loads on the mooring lines were analysed (Figure 9). Nonetheless, a parametric roll of the model ship can be observed for wave periods around 6s, with variations of up to 20°. Pitch angles are more contained, with maximum values of around 4°, whereas peak heave motions can reach values of up to 5m (at full scale). However, these values depend on the specifics of the model ship, and are not fully relevant to the mooring system design, which should be adaptable to any ship within a certain size. Moreover, by looking at the reduced motions, it can be conceived that for those cases that generated the highest loads (Runs 34 and 59), the corresponding motions of the model ship were damped by the mooring system, which is thus fulfilling its function.

In order to further investigate the runs which generated the highest loads on the mooring system, as well as to provide an example of the trends for these loads and the corresponding model ship motions, the loads and DOFs variations for cases 34 and 59 are shown in Figure 12 Figure 15.

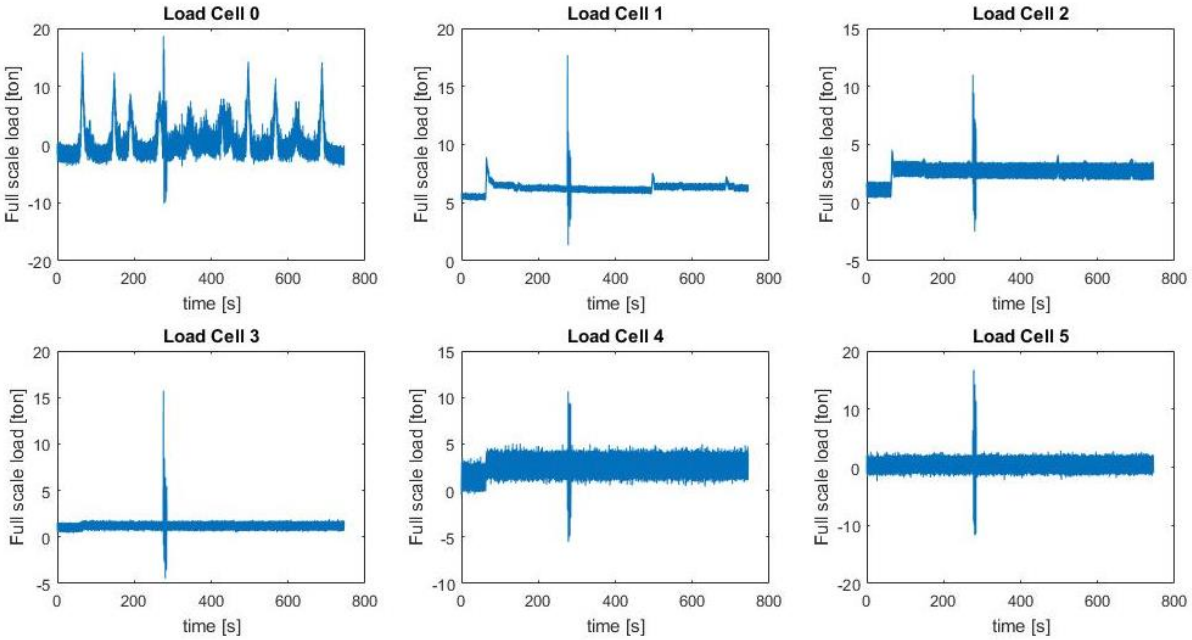

Figure 12. Loads measured for run 34.

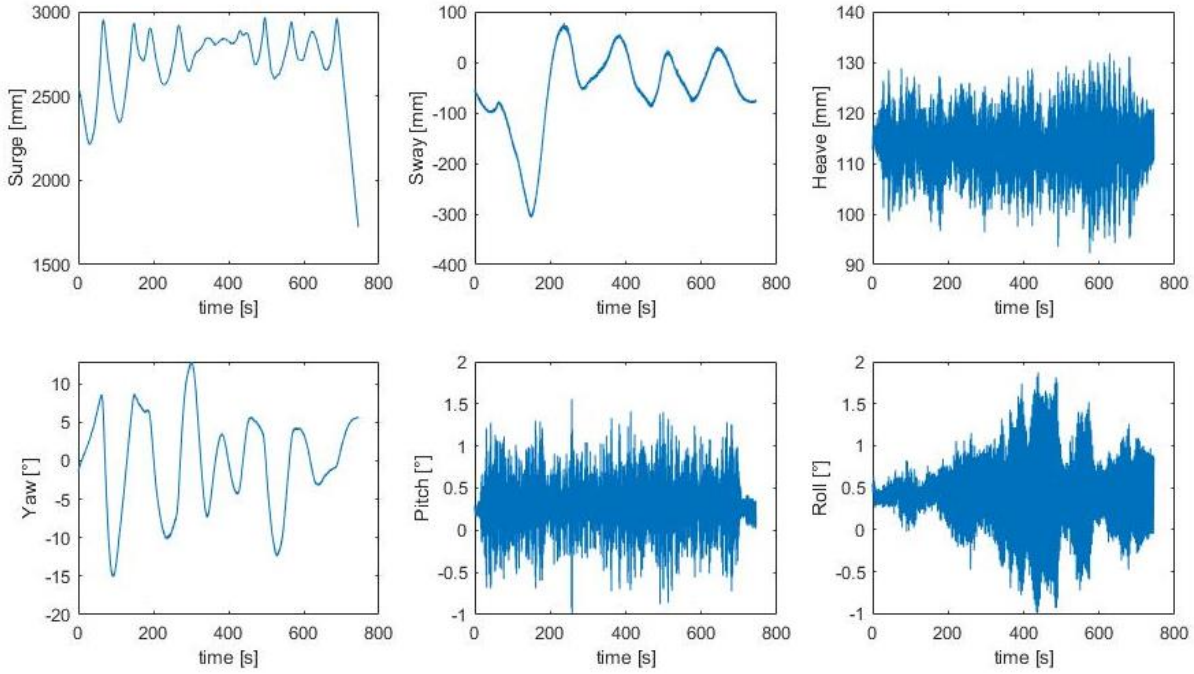

Figure 13. Ship motions measured for run 34.

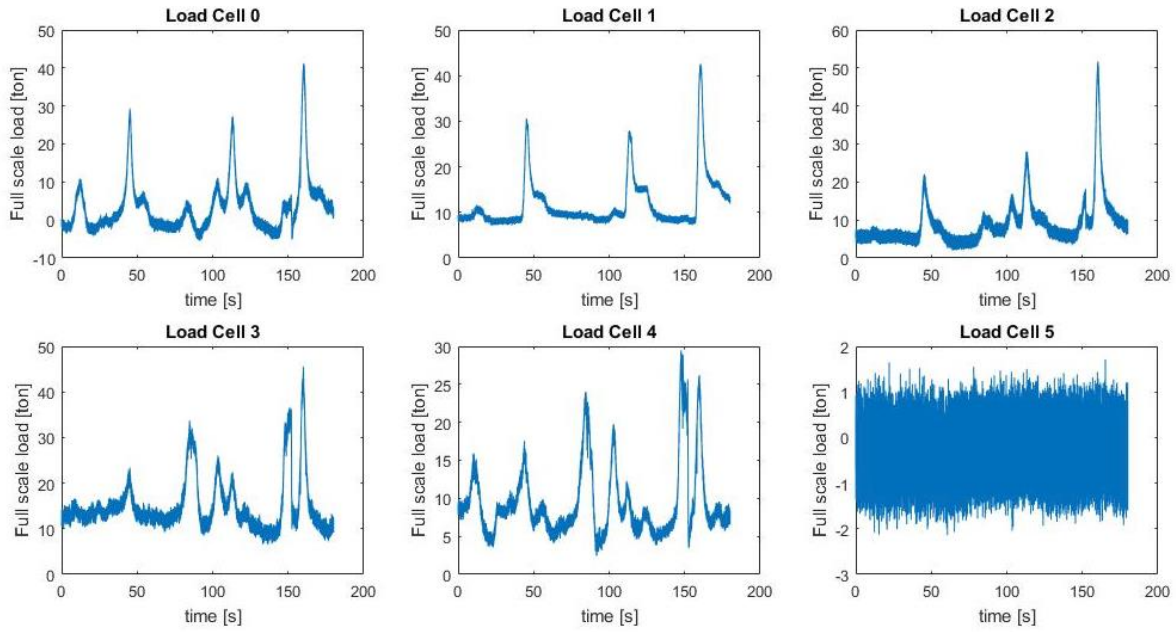

Figure 14. Loads measured for run 59.

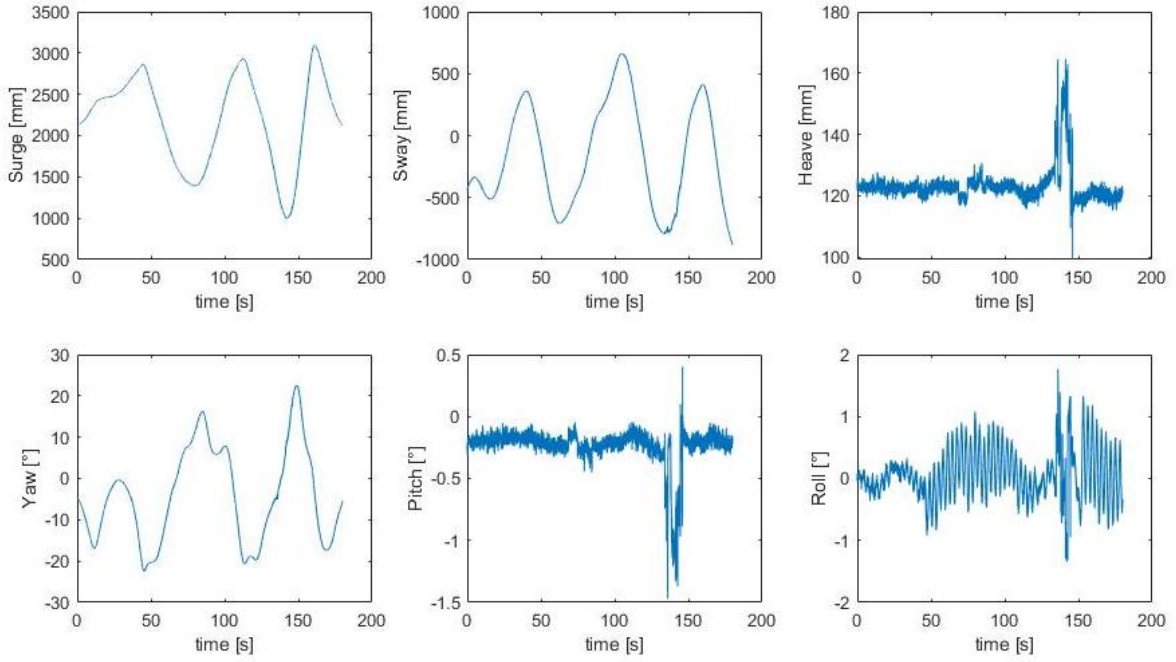

Figure 15. Ship motions measured for run 59.

From these charts (Figure 12 Figure 15) it can be seen how the maximum loads are sometimes determined by instantaneous peaks, e.g. for run 34 in Figure 12, with the average loads being significantly lower. As expected, the loads peaks are detected by all the load cells in correspondence

of the same timesteps, i.e. the same external excitations. This shows that the mooring system works effectively in distributing the loads among all the mooring legs.

In regard to the motions of the model ship, it can be observed that, as expected, the highest motions are those generating the peaks in loads. However, despite heave and pitch motions providing the most significant contribution to the peak loads, it is not possible to identify a single DOF that generates the highest loads. Thus, a combination of motions in all DOFs is likely to generate the peak tensions in the mooring lines.

4 Discussion

The tension estimated with the numerical model on the different sections of the mooring lines falls within the limits established for a satisfactory design, as well as those determined by the mechanical properties of the synthetic material chosen. A minimum number of 8 mooring lines, symmetrically distributed at different angles around the line facing the principal loads direction, is required in order to satisfy station keeping requirements. Similarly, a minimum number of 6 clump weights on the mooring lines facing the loads direction, and 4 on the opposite side, is required to obtain an effective catenary behavior, i.e. a parabolic arch. This was determined by observing the response of the system during both the numerical and experimental tests. A higher number might be considered in order to further reduce the movements of the last weight (the weight closest to the anchor) and thus reduce eventual uplifting forces on the anchors. The simulation shows an effective spread of the tension among the different lines, which aids in the obtainment of a smooth catenary shape for all the lines. This, in turn, allows for a fully horizontal load at the anchor end of the mooring lines, which reduces the holding requirement for the anchors.

From Figure 12 and Figure 14, it can be seen how there is a relatively low reduction between the peak loads detected by load cell 0 (near the central connection ring) and load cell 1 (at the end of the mooring leg facing the coming excitation). This shows that the tension is not significantly reduced along the mooring leg during peak load events. It could be speculated that friction between the granite clump weights and the seabed (which was basically insignificant during the experiments due to the smooth floor of the wave tank) would introduce a damping force able to reduce the tension transmitted to the anchors at the end of the mooring line. However, this same phenomenon had been observed also during the numerical simulations, in which the friction between the clump weights and the seabed had been taken into account using a friction coefficient of 0.55 (see Table 3) according to recommendations available in [22]. Therefore, the numerical model is good at predicting the limited reduction in tension between the first and the last section of the mooring lines. For this reason, anchors should be designed in order to withstand the loads predicted at the beginning of each mooring line. Nonetheless, apart from the peak loads, the mooring system is effective in taking out the low and medium level loads, particularly in the medium load spikes that are observed in load cell 0 but not load cell 1.

A mix of components is chosen according to FHC experience with their existing mooring arrangement, as well as to exploit the properties of the different materials. These are then implemented accordingly in the numerical model. In this regard, the choice of using synthetic ropes might lead to concerns related to friction wear from the seabed, which might cause abrasion and degradation. However, the fact that the lines are positioned at connection points on the clump weights above the seabed, and that noteworthy motions are caused only when significant loads act on

the mooring system, reduces these concerns. If further modelling established that friction were felt to be a concern, the use of a protective jacket for the rope as suggested in [23] could be considered to protect against ingress of small particles likely to cause abrasion. Additionally, the fact that relatively cheap materials are used means that inexpensive repairs can be made either as a consequence of a line's failure or preventatively (either periodically or after inspection). In this regard, one continuous section for each mooring limb, with weights threaded onto it, is suggested instead of shorter independent sections between weights, because eye splices would represent weaker points in the overall structure. Besides, it can be asserted that the choice of using several mooring lines allows also for redundancy in case of failure of one of the sections, e.g. during a storm. Finally, the choice of local material for the anchors and clump weights, such as granite, minimizes environmental impacts and costs of procurement.

A worst case scenario (the unlikely case in which the maximum loads verifiable in the harbour, all coming from same direction, act on the biggest ship for which the mooring system is designed) is chosen as an effective way of designing the system for safe and reliable station-keeping. This is based on the assumption that if the system responds successfully for this worst case, it will behave effectively also for more benign conditions with smaller ships or less significant loads. Despite the hydrodynamic loads acting on large vessels and small crafts can be significantly different, with the mooring design optimized for the worst case scenario, as well as the application of adequate safety factors, the proposed mooring system can be effective also for smaller craft vessels and offshore renewable floating devices (e.g. wave or tidal energy converters). In this regard, as shown during the experimental tests, particular weather conditions which might enable parametric roll, yaw, heave or surge of the moored vessel (i.e. resonance) do not necessarily lead to major loads on the mooring system, which responds effectively to these cases. Nonetheless, more investigation is needed to make sure that the analyses outputs capture the complete range of responses in a long-lasting storm, or when the vessel is not initially aligned to the direction of the environmental loads.

Rather than validating the numerical model, the experimental tests performed in the wave tank served to obtain further insights regarding the dynamic behavior of the mooring system, as well as to demonstrate the effectiveness of the proposed modular design and visualize its response under external excitations in a real environment. The tests explored a wide range of possible situations, with waves up to 2.6m and 11s peak period and currents up to 0.45m/s (at full scale). These conditions exceed typical conditions in Falmouth and other sheltered harbours, giving enough confidence in the suitability of the concept for such environments. In other words, if the numerical model was used to establish a first functioning design, the experimental tests were used to obtain further insights on the behavior of the system.

The performance of the mooring system during the tank tests exceeded the expectations from the numerical modelling. There were no situations in which all the front clump weights (those closest to the central connection ring) were lifted for continuous periods of time, proving the restoring action of the system. Most importantly, the second series of blocks was rarely lifted (only during peak loads) and the third or successive series almost never lifted. This confirmed that the loads observed at the anchor end of the mooring lines were purely horizontal (parallel to the seabed) which is a fundamental requisite for the effective reduction of the anchors requirements. A measure of the tensions, as well as their distribution across the whole system, was obtained and confirmed the effective spreading of load among different lines. This can be used in order to obtain a reliable estimate of full scale loads, which in turn can be used to design the anchor terminations accordingly.

It must be remembered that wind, which is expected to provide a further contribution to the loads acting on the vessel and thus transmitted to the mooring system, could not be included during the experimental trials due to lack of sufficient instrumentation. Thus, current speeds beyond those simulated during the numerical tests were generated in order to prove the effectiveness of the mooring system under more challenging conditions. However, a limitation remains in assessing to what extent the additional current is representative of the aerodynamic forcing caused by the wind loads, and more investigation is needed in this regard.

A last important point for discussion is related to the plausible existence of different sources of error that might have affected the results of both the numerical and experimental investigations. For the numerical modelling, these may concern the modelling of the physical properties of the vessel or of the mooring system components, their interaction with the simulated environment, and the definition of the environmental loads profiles. For the experimental modelling sources of error may include inaccuracies in the scaling of the model components, manual handling and setup of the experimental rig, generation and measurement of the scaled environmental loads during tests. Nonetheless, experts elicitation, preliminary trials and attention to details have been employed throughout the experience in order to minimise the possibility of occurrence of these events.

5 Conclusions

In this work, a novel concept of mooring system based on previous work exploiting the use of clump weights along a mooring line is proposed. As a result, a modular and cost-effective arrangement is presented for application in the offshore renewable energy and commercial moorings sectors. Being a preliminary investigation, the results presented should not be considered as conclusive. However, the outcomes of the numerical and experimental tests confirmed the validity of the concept, and permitted the identification of strengths and areas for improvement of the design.

Future work will consist in further calibrating the numerical model with the results of the experimental tests, in order to improve the capability of designing modular mooring systems for different floating structures and environmental conditions with confidence. To this end, wind loadings could be provisionally removed from the numerical model, or later included in the experimental tests. In addition, a comparison against a conventional system made of steel chains may be used to gain further knowledge on the system's strength and eventual advantages in using synthetic ropes.

Other proposals for future work include the systematic tests for a series of different conditions and vessels or offshore renewable devices. In the last case, additional considerations on the range of motions allowed by the mooring system (e.g. design watch circle) and compatibly with the power extraction principle of the device, should be added to the numerical study. In this regard, the modular configuration of the mooring system allows for an immediate adaptability of its configuration according to both site and device constraints, i.e. the geography of the deployment site or the nature of the moored watercraft. Additionally, an optimization framework could be implemented in order to establish the proper number and distribution of mooring legs and clump weights depending on the metocean conditions of the location in which the mooring system will be deployed. Such tests might include the verification of particular or unusual situations, e.g. the failure of one or multiple mooring lines, or contemplate additional requirements, e.g. minimization of the tilt angle of floating wind platforms. These would also support the calculation of appropriate target safety factors.

Finally, experimental tests could be repeated at full scale in order to get a real representation of the phenomena involved in the system characterization, especially those related to friction with the seabed since these are more difficult to recreate with small scale prototypes. Since a full mooring system would be expensive and impractical to test, the full scale version of a single mooring leg could be recreated instead. In this way, full scale tests in controlled conditions would allow for the quantification of the actual loads at the end of the mooring lines, and therefore establish the required holding power for each individual anchor.

6 Conflict of Interest

The authors declare that the research was conducted in the absence of any commercial or financial relationships that could be construed as a potential conflict of interest.

7 Author Contributions

Conceptualization, G.R., M.S., L.J.; methodology, G.R., M.S., L.J.; data curation, investigation and formal analysis, G.R.; writing, review and editing G.R, T.G., M.S., L.J.; supervision M.S., L.J. All authors have read and agreed to the published version of the manuscript.

8 Funding

This research was funded by the European Union under the European Regional Development Funding (ERDF) Marine-i, grant number 05R16P00381.

9 Acknowledgments

The authors thank the COAST team at the University of Plymouth for the support provided during the experimental tests for this research.

10 References

[1] EMEC. Moorings and Foundations Catalogue, Deliverable 5.1. 2016.

[2] TTI. Moorings & Foundations Analysis of the Innovation Landscape for Cost Reduction in Supporting Infrastructure. 2018.

[3] Weller S, Hardwick J, Johanning L, Karimirad M, Teillant B, Raventos A, et al. A comprehensive assessment of the applicability of available and proposed offshore mooring and foundation technologies and design tools for array applications. 2014.

[4] Carbon Trust. Floating Wind Joint Industry Project Phase I Summary Report. 2018.

[5] Skop RA. Mooring Systems: A state-of-the-art review. J Offshore Mech Arct Eng 1988;110:365–72. https://doi.org/https://doi.org/10.1115/1.3257074.

[6] Harris R, Johanning L, Wolfram J. Mooring systems for wave energy converters: A review of design issues and choices. 3rd Int. Conf. Mar. Renew. Energy, 2004, p. 180–9.

[7] Yuan ZM, Incecik A, Ji C. Numerical study on a hybrid mooring system with clump weights

and buoys. Ocean Eng 2014;88:1–11. https://doi.org/10.1016/j.oceaneng.2014.06.002.

[8] Falmouth Harbour Commissioners (FHC) n.d. https://www.falmouthharbour.co.uk/ (accessed January 7, 2020).

[9] Weller SD, Johanning L, Davies P, Banfield SJ. Synthetic mooring ropes for marine renewable energy applications. Renew Energy 2015;83:1268–78. https://doi.org/10.1016/j.renene.2015.03.058.

[10] Weller SD, Davies P, Vickers AW, Johanning L. Synthetic rope responses in the context of load history: The influence of aging. Ocean Eng 2015;96:192–204. https://doi.org/https://doi.org/10.1016/j.oceaneng.2014.12.013.

[11] Chun yan J, Zhi ming Y, Ming lu C. Study on a new mooring system integrating catenary with taut mooring. China Ocean Eng 2011;25:427–40. https://doi.org/10.1007/s13344-011-0035-4.

[12] Ma K, Shu H, Smedley P, L'Hostis D, Duggal A. A Historical Review on Integrity Issues of Permanent Mooring Systems. Offshore Technol Conf 2013:14. https://doi.org/10.4043/24025-MS.

[13] Chunyan J, Zhiming Y. Experimental study of a hybrid mooring system. J Mar Sci Technol 2015;20:213–25. https://doi.org/10.1007/s00773-014-0260-7.

[14] Chakrabarti S, Halkyard J, Capanoglu C. Historical Development of Offshore Structures. Handb Offshore Eng 2005:1–38. https://doi.org/10.1016/B978-008044381-2.50004-7.

[15] OrcaFlex documentation n.d. https://www.orcina.com/resources/documentation/ (accessed January 7, 2020).

[16] Thomsen JB, Ferri F, Kofoed JP. Screening of available tools for dynamic mooring analysis of wave energy converters. Energies 2017;10. https://doi.org/10.3390/en10070853.

[17] Bexco catalogue 2019. https://www.bexco.be/offshorerope (accessed January 7, 2020).

[18] Marlow catalogue 2019. www.marlowropes.com (accessed January 7, 2020).

[19] Thomsen JB, Ferri F, Kofoed JP. Validation of a tool for the initial dynamic design of mooring systems for large floating wave energy converters. J Mar Sci Eng 2017;5:1–23. https://doi.org/10.3390/jmse5040045.

[20] Harnois V, Weller SD, Johanning L, Thies PR, Le Boulluec M, Le Roux D, et al. Numerical model validation for mooring systems: Method and application for wave energy converters. Renew Energy 2015;75:869–87. https://doi.org/10.1016/j.renene.2014.10.063.

[21] COAST Laboratory - University of Plymouth n.d. https://www.plymouth.ac.uk/research/institutes/marine-institute/coast-laboratory (accessed January 7, 2020).

[22] Taylor R, Valent P. Design Guide for Drag Embedment Anchors. 1984.

[23] Gordelier T, Parish D, Thies RP, Johanning L. A Novel Mooring Tether for Highly-Dynamic

Offshore Applications; Mitigating Peak and Fatigue Loads via Selectable Axial Stiffness. J Mar Sci Eng 2015;3. https://doi.org/10.3390/jmse3041287.

APPENDIX - Wave tank test cases specifications

Table A1. Test cases with regular waves only.

	Full Scale		Model Scale	
Run	T [s]	H [m]	T [s]	H [m]
Run_001	4.0	1.2	0.73	0.040
Run_002	4.2	1.2	0.77	0.040
Run_003	4.4	1.2	0.80	0.040
Run_004	4.6	1.2	0.84	0.040
Run_005	4.8	1.2	0.88	0.040
Run_006	5.0	1.2	0.91	0.040
Run_007	5.2	1.2	0.95	0.040
Run_008	5.4	1.2	0.99	0.040
Run_009	5.6	1.2	1.02	0.040
Run_010	5.8	1.2	1.06	0.040
Run_011	6.0	1.2	1.10	0.040
Run_012	6.2	1.2	1.13	0.040
Run_013	6.4	1.2	1.17	0.040
Run_014	6.6	1.2	1.20	0.040
Run_015	6.8	1.2	1.24	0.033
Run_016	7.0	1.2	1.28	0.040
Run_017	7.2	1.2	1.31	0.040
Run_018	7.4	1.2	1.35	0.040
Run_019	7.6	1.2	1.39	0.040
Run_020	7.8	1.2	1.42	0.040
Run_021	8.0	1.2	1.46	0.040
Run_022	8.2	1.2	1.50	0.040
Run_023	8.4	1.2	1.53	0.040
Run_024	8.6	1.2	1.57	0.040
Run_025	8.8	1.2	1.61	0.040
Run_026	9.0	1.2	1.64	0.040
Run_027	9.2	1.2	1.68	0.040
Run_028	9.4	1.2	1.72	0.040
Run_029	9.6	1.2	1.75	0.040
Run_030	9.8	1.2	1.79	0.040
Run_031	10.0	1.2	1.83	0.040

Table A2. Test cases with irregular waves only.

	Full Scale			Model Scale			
	Tz [s]	Tp [s]	Hs [m]	Tz [s]	Tp [s]	Hs [m]	Gamma
Run_032	4	5.16	1.2	0.73	0.94	0.040	3.3
Run_033	5	6.45	1.6	0.91	1.18	0.053	3.3
Run_034	6	7.74	2	1.10	1.41	0.067	3.3
Run_035	7	9.03	2.2	1.28	1.65	0.073	3.3
Run_036	8	10.32	2.4	1.46	1.88	0.080	3.3
Run_037	9	11.61	2.6	1.64	2.12	0.087	3.3

Table A3. Test cases with irregular waves and current.

	Full Scale				Model Scale			
	Tz [s]	Tp [s]	Hs [m]	Current [m/s]	Tz [s]	Tp [s]	Hs [m]	Current [m/s]
Run_038				0.3				0.055
Run_039	4	5.16	1.2	0.3	0.73	0.94	0.040	0.055
Run_040	5	6.45	1.6	0.3	0.91	1.18	0.053	0.055
Run_041	6	7.74	2	0.3	1.10	1.41	0.067	0.055
Run_042	7	9.03	2.2	0.3	1.28	1.65	0.073	0.055
Run_043	8	10.32	2.4	0.3	1.46	1.88	0.080	0.055
Run_044	9	11.61	2.6	0.3	1.64	2.12	0.087	0.055
Run_045				0.45				0.082
Run_046	4	5.16	1.2	0.45	0.73	0.94	0.040	0.082
Run_047	9	11.61	2.6	0.45	1.64	2.12	0.087	0.082
Run_048	5	6.45	1.6	0.45	0.91	1.18	0.053	0.082
Run_049	6	7.74	2	0.45	1.10	1.41	0.067	0.082
Run_050	7	9.03	2.2	0.45	1.28	1.65	0.073	0.082
Run_051	8	10.32	2.4	0.45	1.46	1.88	0.080	0.082
Run_060	9	11.61	2.6	1.3	1.64	2.12	0.087	0.237

Table A4. Test cases with current only.

	Full Scale	Model Scale
Run	Flow Speed [m/s]	Flow Speed [m/s]
Run_052	0.549256181	0.100
Run_053	0.823884271	0.150
Run_054	1.098512361	0.201
Run_055	1.373140452	0.251
Run_056	1.647768542	0.301
Run_057	1.922396632	0.351

Run_058	2.197024723	0.401
Run_059	2.471652813	0.451